research papers

BIOLOGICAL CRYSTALLOGRAPHY

ISSN: 1399-0047

Volume 68 | Part 9 | September 2012 | Pages 1189-1193
https://doi.org/10.1107/S0907444912024080
Cited by 3

Structural analysis of the Asn152Gly mutant of P99 cephalosporinase

James F. Ruble,[a] Scott T. Lefurgy,[b]‡ Virginia W. Cornish[b] and Rachel A. Powers[a]*

[a]Department of Chemistry, Grand Valley State University, 1 Campus Drive, Allendale, MI 49401, USA, and [b] Department of Chemistry, Columbia University, 3000 Broadway, New York, NY 10027, USA
*Correspondence e-mail: powersra@gvsu.edu

(Received 21 February 2012; accepted 26 May 2012; online 18 August 2012)

P99 cephalosporinase is a class C β-lactamase that is responsible in part for the widespread bacterial resistance to β-lactam antibiotics. Mutations of the conserved active-site residue Asn152 of the enzyme have been shown to alter β-lactam substrate specificity *in vivo*. Mutation of Asn152 to a glycine is notable in that it exhibits *in vivo* substrate-selectivity switching. In order to better understand the structural basis for this observed switch, the X-ray crystal structure of the apo Asn152Gly mutant of P99 was determined to 1.95 Å resolution. Unexpectedly, the artificial C-terminal His_6 tag of a symmetrically-related molecule was observed bound in the active site. The His_6 tag makes several interactions with key active-site residues, as well as with several sulfate ions. Additionally, the overall C-terminus occupies the space left vacant upon the mutation of Asn152 to glycine.

Keywords: **P99**; **cephalosporinase**; **β-lactamases**; **mutant enzymes**; **His_6 tag**; **antibiotic resistance**; **extended spectrum**.

3D view: 3s4x

PDB reference: P99 cephalosporinase, Asn152Gly mutant, 3s4x

1. Introduction

Antibiotic resistance has emerged as one of the leading public health crises of the 21st century (Neu, 1992; Davies & Davies, 2010). Many resistant bacteria express the enzyme β-lactamase, the most widespread resistance mechanism to β-lactam antibiotics. β-Lactams such as penicillin and the cephalosporins are the most widely prescribed class of antibiotics in clinical use. β-Lactamases cleave the defining lactam ring, rendering the antibiotic inactive against its original cellular target, the cell-wall transpeptidase enzymes.

β-Lactamases are categorized into four classes (A–D), each exhibiting a unique mechanism for destruction of β-lactam substrates (Bush *et al.*, 1995; Fisher *et al.*, 2005). The class C β-lactamase from *Enterobacter cloacae* strain P99 (referred to as P99) is traditionally known as a cephalosporinase for its preferred substrates, first-generation cephalosporins. An extended-spectrum β-lactamase (ESBL), a natural mutant of P99, has been isolated from *E. cloacae* strain GC1 (Nukaga *et al.*, 1995). The observed extended-spectrum activity of this enzyme against third-generation cephalosporins is the consequence of a three-amino-acid insertion in the Ω-loop (residues 189–226) of the enzyme. This enlarges the active site of the enzyme and better accommodates the bulkier R_1 side chains of this class of molecules (Crichlow *et al.*, 1999; Nukaga *et al.*, 2004). Hydrolysis of third-generation cephalosporins can also be accomplished when the R2 loop (residues 289–307) is disrupted. Deletions or insertions of between two and six residues in this loop have been identified as causes of extended-spectrum activity in plasmid-encoded class C enzymes, in natural variants and in clinical isolates (Barnaud *et al.*, 2001; Doi *et al.*, 2004; Mammeri *et al.*, 2004, 2007; Lee *et al.*, 2004). The R2 loop accommodates the R_2 side chains of cephalosporins and the crystal structures of several class C ESBLs have confirmed that the R2 site is enlarged compared with non-ESBL enzymes (Kim *et al.*, 2006; Yamaguchi *et al.*, 2009).

Site-saturation mutagenesis at position 152 of the P99 β-lactamase identified three mutants that exhibit a substrate-selectivity switch with a single amino-acid change (Lefurgy *et al.*, 2007). Asn152 is a completely conserved residue among class C β-lactamases and, although it does not actively participate in destruction of the β-lactam, it is instrumental in appropriately positioning the β-lactam in the active site by hydrogen bonding to the R_1 amide group common to many β-lactam antibiotics (Dubus *et al.*, 1995). Additionally, it is a central residue in an elaborate hydrogen-bonding network found in the active sites of the class C enzymes. In the structure of the wild-type P99 enzyme, the Asn152 side chain hydrogen bonds to Lys67 and Gln120, both of which are also completely conserved residues in class C enzymes (Lobkovsky *et al.*, 1993).

Three individual point mutations at this position have been shown to retain activity yet display a significantly altered substrate profile: Asn152Ser, Asn152Thr and Asn152Gly (Lefurgy *et al.*, 2007). Of these three, the glycine mutant was active towards penicillin G, ampicillin, oxacillin and cephalothin, picking up efficiency toward oxacillin at the expense of efficiency towards cefotaxime and cefoxitin

elimination of a side chain at this position. In an effort to explain the structural basis of the observed substrate-selectivity switch, we determined the X-ray crystal structure of the Asn152Gly mutant of the class C β-lactamase from *E. cloacae* P99 to 1.95 Å resolution.

2. Materials and methods

2.1. Expression and purification of Asn152Gly P99 β-lactamase

Expression and purification of the Asn152Gly mutant P99 β-lactamase was performed as described previously (Lefurgy *et al.*, 2007). Briefly, *Escherichia coli* cells containing the pET26b plasmid for the Asn152Gly mutant were inoculated into an overnight starter culture of 2×YT supplemented with 0.025 mg ml^{-1} kanamycin and grown at 310 K to an optical density of 0.6 measured at 600 nm. Expression was induced with 100 µ*M* isopropyl β-D-1-thiogalactopyranoside (IPTG) for 4 h at 310 K. The cultures were harvested by centrifugation and the cell pellets were stored at 193 K. Frozen cell pellets were thawed on ice and resuspended in a buffer consisting of 20 m*M* Tris–HCl, 500 m*M* NaCl, 5 m*M* imidazole pH 8.0. Cells were lysed using sonication and then centrifuged to remove cellular debris. The Asn152Gly enzyme was purified *via* affinity chromatography using Ni–NTA Superflow resin (Qiagen, Valencia, California, USA) to bind the engineered C-terminal histidine (His_6) tag. The enzyme was eluted with a linear gradient of 5–200 m*M* imidazole and subsequently dialyzed into phosphate-buffered saline. Purity was verified using SDS–PAGE and Western blotting with an antibody against the His_6 tag. Absorbance measurements at 280 nm were performed to calculate the purified enzyme concentration using a molar extinction coefficient of 71 000 M^{-1} cm^{-1}.

2.2. Crystallization and structure determination

A Phoenix high-throughput crystallization robot (Van Andel Research Institute, Grand Rapids, Michigan, USA) was used to identify initial crystallization conditions, which were subsequently optimized using hanging-drop vapor diffusion. The mother liquor consisted of 0.15 *M* ammonium sulfate, 30% polyethylene glycol (PEG) 8000, pH 6.5. Drops of 5 µl were set up using enzyme at a concentration of 3.5 mg ml^{-1} diluted in a 1:1 ratio with mother liquor. Crystals grew at room temperature and appeared in approximately one week. Diffraction data were collected on the LS-CAT beamline (21-ID-D) at the Advanced Photon Source, Argonne, Illinois, USA at 100 K using a MAR CCD detector. Prior to data collection, the crystal was soaked in a solution containing 40% PEG 8000 as a cryoprotectant before flash-cooling in liquid nitrogen.

Reflections were indexed, integrated and scaled using *HKL*-2000 (Otwinowski & Minor, 1997). The space group was $P2_12_12$, with one P99 monomer in the asymmetric unit. The structure was determined with *Phaser* (McCoy *et al.*, 2007) using the *A* monomer of wild-type P99 (PDB entry 1xx2 ; Lobkovsky *et al.*, 1993) as the initial phasing model (all water molecules were removed). Refinement and electron-density map calculations were performed with *REFMAC*5 (Murshudov *et al.*, 2011) in the *CCP*4 program suite (Winn *et al.*, 2011). Manual rebuilding of the model was performed with *Coot* (Emsley & Cowtan, 2004). The final model contained 367 residues, which included the C-terminal His_6 tag, 221 water molecules and seven sulfate ions. The coordinates for this structure have been deposited in the Protein Data Bank as entry 3s4x .

3. Results and discussion

3.1. Structure of Asn152Gly P99 β-lactamase

Optimization of the conditions identified from the screens ultimately led to the determination of the structure of the Asn152Gly mutant of P99 β-lactamase to 1.95 Å resolution. Inspection of the initial $F_o - F_c$ difference maps revealed significant electron density contoured at 3σ present in the active site of the enzyme. Attempts to identify this density as a buffer molecule or an additive in the crystallization conditions proved to be unsuccessful. However, when symmetry-related molecules were displayed it was readily apparent that the density was continuous with the C-terminus of a symmetry mate. This density was subsequently modeled as the engineered C-terminal His_6 tag (residues 362–367) used in the purification process (Fig. 1). The side chains of all of the histidines were visible, with the exception of His363, for which no density was observed beyond the C^β atom. The presence of the His_6 tag in the active site was unexpected and efforts to displace it through soaking of substrates were unsuccessful, with the crystals dissolving rapidly during the soaking process. The Asn152Gly construct used here lacked a protease cleavage site prior to the C-terminal His_6 tag, thereby preventing its removal. Crystallization attempts using an Asn152Gly construct that did not contain an affinity tag have so far been unsuccessful.

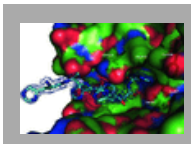

Figure 1
Binding of the His_6 tag in the active site of the Asn152Gly P99 β-lactamase mutant. $2F_o - F_c$ electron-density map of the bound His_6 tag contoured at 1.0σ. This and all subsequent figures were made with *PyMOL* (DeLano, 2002).

Three sulfate ions were observed to be bound in the active site, spanning nearly the entire length of the His_6 tag and interacting extensively with several of the histidines (Fig. 2). These ions also interact with active-site residues Ser64, Tyr150, Ser212, Lys315, Thr316 and Gly320 (Fig. 2). His366 is also involved in π–π stacking interactions with Tyr221. The interactions observed between the enzyme and both the His_6 tag and the sulfate ions allow a better understanding of the types of ligands that may be accommodated in this active site. The quality of the final model was analyzed with the program *MolProbity* (Chen *et al.*, 2010): 98.4% of all residues

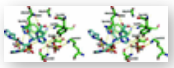

Figure 2
Stereoview of the interactions in the active site of the Asn152Gly mutant. C atoms of the His_6 tag are colored cyan, C atoms of the rest of the protein are colored green, N atoms blue, O atoms red and S atoms orange. Water molecules are represented as red spheres. Hydrogen bonds are shown as yellow dashed lines and represent distances between 2.5 and 3.2 Å.

3.2. Comparison with wild-type P99 β-lactamase

The crystals of the Asn152Gly mutant were grown under conditions that differed from those used for the wild-type P99 enzyme and resulted in a structure with a different space group (data for the mutant are given in Table 1; the wild-type crystal belonged to space group $P2_1$) and unit-cell parameters (Table 1; the wild-type crystal had unit-cell parameters a = 46.50, b = 83.47, c = 95.46 Å, β = 90°). Additionally, the mutant contained a monomer in the asymmetric unit, whereas the wild-type structure crystallized with a dimer in the asymmetric unit. Superposition of the Asn152Gly mutant structure with the wild-type enzyme (PDB entry 1xx2 ; Lobkovsky *et al.*, 1993) indicated that there were no major changes in the overall fold of the mutant enzyme. The r.m.s.d. between all C^{α} atoms common to the two structures was 0.4 Å, with most of the differences occurring in the loop containing Gln120 and the helix (helix H4a) that immediately follows.

Table 1
Crystallographic summary for the structure of the Asn152Gly mutant of P99

Values in parentheses are for the highest resolution shell.

Unit-cell parameters (Å, °)	a = 78.96, b = 85.48, c = 51.68, α = 90, β = 90, γ = 90
Space group	$P2_12_12$
Resolution (Å)	1.95 (2.02–1.95)
Unique reflections	25774
Total observations	115550
R_{merge} (%)	10.4 (37.1)
Completeness† (%)	98.3 (98.1)
$\langle I/\sigma(I)\rangle$	8.6 (4.8)
Resolution range for refinement (Å)	35–1.95
No. of protein residues	367
No. of water molecules	221
R.m.s.d. bond lengths (Å)	0.023
R.m.s.d bond angles (°)	1.3
R factor (%)	17.6
R_{free}‡ (%)	23.4
Average B factor (Å^2)	
Protein atoms	29.3
Water molecules	34.7
His_6 tag	47.8

†Fraction of theoretically possible reflections observed.
‡R_{free} was calculated using 5% of reflections that were set aside randomly.

3.3. Active site of the Asn152Gly mutant

Several changes are observed within the active-site architecture of the mutant compared with wild-type P99. The first is the disruption of the extensive hydrogen-bonding network found in the active sites of the class C β-lactamase enzymes, which is a consequence of the loss of the hydrophilic Asn152 side chain. Asn152 is centrally located in the active site. In addition to hydrogen bonding to the conserved residues Gln120 and Lys67, Asn152 is believed to help position the β-lactam substrate in the active site by forming a hydrogen bond to the conserved R_1 amide group of the β-lactam antibiotic (Patera *et al.*, 2000; Powers *et al.*, 2001; Oefner *et al.*, 1990; Dubus *et al.*, 1995). With the entire side chain of Asn152 removed in the Asn152Gly mutant, Gln120 has lost its hydrogen-bonding partner and as a result the Gln120 side chain has flipped out from its `wild-type' conformation. Gln120 $O^{\epsilon 1}$ now forms hydrogen bonds to the main-chain N atoms of the last two residues of the His_6 tag (His366 and His367), and Gln120 $N^{\epsilon 1}$ interacts with a water molecule (Wat68).

Another residue involved in the hydrogen-bond network surrounding Asn152 is the conserved Lys67. In the wild-type enzyme a hydrogen bond is observed between Asn152 $O^{\delta 1}$ and Lys67 N^{ζ}. Upon mutation to glycine this interaction cannot occur, but the conformation of Lys67 remains relatively unchanged owing to interaction with the His_6 tag. Interestingly, the carboxylate group of the overall C-terminus of the monomer (*i.e.* of His367) occupies the `hole' left by the mutation of Asn152 to glycine (Fig. 3). The carboxylate group is in a similar position to the amide group in the side chain of Asn152 in the wild-type structure. This carboxylate-binding site is unique to the Asn152Gly mutant and is distinct from the binding site that recognizes the C4 carboxylate of cephalosporin antibiotics (Powers & Shoichet, 2002). In the Asn152Gly mutant structure one of the O atoms of this carboxylate (OXT; average B factor 41.7 Å^2) serves as a replacement hydrogen-bonding partner with Lys67 N^{ζ} (average B factor 29.1 Å^2). The other carboxylate O atom (O; average B factor 41.2 Å^2) makes a hydrogen bond to Wat64 (average B factor 38.8 Å^2).

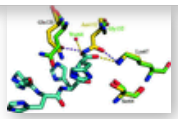

Superposition of the Asn152Gly mutant with wild-type P99 β-lactamase (PDB entry 1xx2). Hydrogen bonds observed in the mutant are shown as yellow dashed lines and those in wild-type P99 are shown in magenta. Atoms are colored as in Fig. 2, except that the C atoms of the wild-type P99 enzyme are colored yellow.

A more dramatic change in the active site is the apparent `closing' of the active site around the inserted His_6 tag. Secondary-structure matching (SSM) of the Asn152Gly mutant structure with both apo wild-type P99 (PDB entry 1xx2) and wild-type P99 in complex with a phosphonate inhibitor (PDB entry 1bls ; Lobkovsky *et al.*, 1994) was performed in *Coot* (Emsley & Cowtan, 2004), with a resulting r.m.s.d. of 0.43 Å for 359 common amino-acid residues. When compared with the wild-type P99 structure, shifts in C^{α}-atom positions of approximately 1 Å are observed in the loop that includes residues 117–127 and residues 128–138 of the subsequent helix H4a in the Asn152Gly mutant (Fig. 4). The overall effect of the shift is a closing of these regions around the His_6 tag. This same closure is not observed when comparing the Asn152Gly mutant structure with the phosphonate-bound complex (PDB entry 1bls), in which these regions superpose well with the apo wild-type P99 structure. Therefore, this `closing' effect seems most likely to arise from the presence of the His_6 tag, which is a crystallographic artifact of this structure. The observed smaller active site is in contrast to most ESBL structures, which reveal an increase in the size of the active site upon mutation, thereby making these enzymes better able to accommodate bulkier antibiotics. The conformational flexibility observed in this region of Asn152Gly suggests that this might be another area that may allow an increase in the size of the active site and allow extended-spectrum activity with a single amino-acid change. A structure of Asn152Gly in complex with a β-lactam such as oxacillin would shed light on this possibility. From a drug-design perspective, the presence of the His_6 tag and three sulfate ions bound in the active site of this mutant also provides insight into the binding capabilities in the active site and may aid in future inhibitor design.

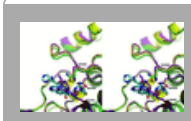

Figure 4
Closure of the Asn152Gly active site around the His_6 tag. Superposition of the Asn152Gly mutant with wild-type apo P99 β-lactamase (PDB entry 1xx2) and wild-type P99 β-lactamase in complex with a phosphonate inhibitor (PDB entry 1bls). Atoms are colored as in Fig. 3, except that the C atoms of the wild-type P99 complex are colored magenta. Helix H4a is labeled, as is the loop containing Gln120.

Given the observed His_6 tag in the active site of the Asn152Gly mutant, it is conceivable that a free His_6 or similar polypeptide might act as an inhibitor of this P99 structural variant. While this possibility exists, it should be noted that, prior to knowledge of the bound His_6 tag, soaking the Asn152Gly crystals in cryoprotectant solution containing a saturating concentration of oxacillin resulted in rapid crystal degradation, implying that a significant contribution to this interaction arises as an artifact of the crystallization process itself. Nevertheless, this would be an interesting question to address, specifically with regard to the sequence specificity of the polypeptide.

Supporting information

3D view: 3s4x

PDB reference: P99 cephalosporinase, Asn152Gly mutant, 3s4x

Footnotes

‡Present address: Department of Chemistry, 106A Berliner Hall, 151 Hofstra University, Hempstead, NY 11549, USA.

Acknowledgements

This research was supported by a Cottrell College Science Award from Research Corporation and an NSF-Advance professional development grant (to RAP). The authors would like to acknowledge Eric Xu at the Van Andel Research Institute, Grand Rapids, Michigan for use of the Phoenix crystallization robot. Use of the Advanced Photon Source was supported by the US Department of Energy, Office of Science, Office of Basic Energy Sciences under Contract No. DE-AC02-06CH11357. Use of LS-CAT Sector 21 was supported by the Michigan Economic Development Corporation and the Michigan Technology Tri-Corridor for the support of this research program (Grant 085P1000817).

References

Barnaud, G., Labia, R., Raskine, L., Sanson-Le Pors, M. J., Philippon, A. & Arlet, G. (2001). *FEMS Microbiol. Lett.* **195**, 185–190. Web of Science CrossRef PubMed CAS Google Scholar

Chen, V. B., Arendall, W. B., Headd, J. J., Keedy, D. A., Immormino, R. M., Kapral, G. J., Murray, L. W., Richardson, J. S. & Richardson, D. C. (2010). *Acta Cryst.* D**66**, 12–21. Web of Science CrossRef CAS IUCr Journals Google Scholar

Crichlow, G. V., Kuzin, A. P., Nukaga, M., Mayama, K., Sawai, T. & Knox, J. R. (1999). *Biochemistry*, **38**, 10256–10261. Web of Science CrossRef PubMed CAS Google Scholar

Davies, J. & Davies, D. (2010). *Microbiol. Mol. Biol. Rev.* **74**, 417–433. Web of Science CrossRef CAS PubMed Google Scholar

DeLano, W. L. (2002). *PyMOL*. http://www.pymol.org . Google Scholar

Doi, Y., Wachino, J., Ishiguro, M., Kurokawa, H., Yamane, K., Shibata, N., Shibayama, K., Yokoyama, K., Kato, H., Yagi, T. & Arakawa, Y. (2004). *Antimicrob. Agents Chemother.* **48**, 2652–2658. Web of Science CrossRef PubMed CAS Google Scholar

Dubus, A., Normark, S., Kania, M. & Page, M. G. (1995). *Biochemistry*, **34**, 7757–7764. CrossRef CAS PubMed Web of Science Google Scholar

Emsley, P. & Cowtan, K. (2004). *Acta Cryst.* D**60**, 2126–2132. Web of Science CrossRef CAS IUCr Journals Google Scholar

Fisher, J. F., Meroueh, S. O. & Mobashery, S. (2005). *Chem. Rev.* **105**, 395–424. Web of Science CrossRef PubMed CAS Google Scholar

Kim, J. Y., Jung, H. I., An, Y. J., Lee, J. H., Kim, S. J., Jeong, S. H., Lee, K. J., Suh, P.-G., Lee, H.-S., Lee, S. H. & Cha, S.-S. (2006). *Mol. Microbiol.* **60**, 907–916. Web of Science CrossRef PubMed CAS Google Scholar

Lee, J. H., Jung, H. I., Jung, J. H., Park, J. S., Ahn, J. B., Jeong, S. H., Jeong, B. C., Lee, J.-H. & Lee, S. H. (2004). *Microb. Drug Resist.* **10**, 224–230. Web of Science CrossRef PubMed CAS Google Scholar

Lefurgy, S. T., de Jong, R. M. & Cornish, V. W. (2007). *Protein Sci.* **16**, 2636–2646. Web of Science CrossRef PubMed CAS Google Scholar

Lobkovsky, E., Billings, E. M., Moews, P. C., Rahil, J., Pratt, R. F. & Knox, J. R. (1994). *Biochemistry*, **33**, 6762–6772. CrossRef CAS PubMed Web of Science Google Scholar

Lobkovsky, E., Moews, P. C., Liu, H., Zhao, H., Frere, J.-M. & Knox, J. R. (1993). *Proc. Natl Acad. Sci. USA*, **90**, 11257–11261. CrossRef CAS PubMed Web of Science Google Scholar

Mammeri, H., Poirel, L., Bemer, P., Drugeon, H. & Nordmann, P. (2004). *Antimicrob. Agents Chemother.* **48**, 716–720. Web of Science CrossRef PubMed CAS Google Scholar

Mammeri, H., Poirel, L. & Nordmann, P. (2007). *J. Antimicrob. Chemother.* **60**, 490–494. Web of Science CrossRef PubMed CAS Google Scholar

McCoy, A. J., Storoni, L. C. & Read, R. J. (2007). *Evolving Methods for Macromolecular Crystallography*, edited by R. J. Read & J. L. Sussman, pp. 67–77. Dordrecht: Springer. Google Scholar

Murshudov, G. N., Skubák, P., Lebedev, A. A., Pannu, N. S., Steiner, R. A., Nicholls, R. A., Winn, M. D., Long, F. & Vagin, A. A. (2011). *Acta Cryst.* D**67**, 355–367. Web of Science CrossRef CAS IUCr Journals Google Scholar

Neu, H. C. (1992). *Science*, **257**, 1064–1073. CrossRef PubMed CAS Web of Science Google Scholar

Nukaga, M., Haruta, S., Tanimoto, K., Kogure, K., Taniguchi, K., Tamaki, M. & Sawai, T. (1995). *J. Biol. Chem.* **270**, 5729–5735. CrossRef CAS PubMed Google Scholar

Nukaga, M., Kumar, S., Nukaga, K., Pratt, R. F. & Knox, J. R. (2004). *J. Biol. Chem.* **279**, 9344–9352. Web of Science CrossRef PubMed CAS Google Scholar

Oefner, C., D'Arcy, A., Daly, J. J., Gubernator, K., Charnas, R. L., Heinze, I., Hubschwerlen, C. & Winkler, F. K. (1990). *Nature (London)*, **343**, 284–288. CrossRef CAS PubMed Web of Science Google Scholar

Otwinowski, Z. & Minor, W. (1997). *Methods Enzymol.* **276**, 307–326. CrossRef CAS Web of Science Google Scholar

Patera, A., Blaszczak, L. C. & Shoichet, B. K. (2000). *J. Am. Chem. Soc.* **122**, 10504–10512. Web of Science CrossRef CAS Google Scholar

Powers, R. A., Caselli, E., Focia, P. J., Prati, F. & Shoichet, B. K. (2001). *Biochemistry*, **40**, 9207–9214. Web of Science CrossRef PubMed CAS Google Scholar

Powers, R. A. & Shoichet, B. K. (2002). *J. Med. Chem.* **45**, 3222–3234. Web of Science CrossRef PubMed CAS Google Scholar

Winn, M. D. *et al.* (2011). *Acta Cryst.* D**67**, 235–242. Web of Science CrossRef CAS IUCr Journals Google Scholar

Yamaguchi, Y., Sato, G., Yamagata, Y., Doi, Y., Wachino, J., Arakawa, Y., Matsuda, K. & Kurosaki, H. (2009). *Acta Cryst.* F**65**, 540–543. Web of Science CrossRef IUCr Journals Google Scholar

BIOLOGICAL CRYSTALLOGRAPHY

ISSN: 1399-0047

Volume 68 | **Part 9** | September 2012 | Pages 1189-1193
https://doi.org/10.1107/S0907444912024080